

Article

Towards a Standard Plant Species Spectral Library Protocol for Vegetation Mapping: A Case Study in the Shrubland of Doñana National Park

Marcos Jiménez ^{1,*} and Ricardo Díaz-Delgado ²

¹ Remote Sensing Area, National Institute of Aerospace Technologies (INTA), Ctra. Ajalvir s/n, Torrejón de Ardoz, 28850 Madrid, Spain

² Remote Sensing and GIS Lab., Doñana Biological Station, CSIC, Avda. Americo Vespucio, 41092 Sevilla, Spain; E-Mail: rdiaz@ebd.csic.es

* Author to whom correspondence should be addressed; E-Mail: jimenezmm@inta.es; Tel.: +34-915-201-989; Fax: +34-915-201-963.

Academic Editor: Wolfgang Kainz

Received: 11 August 2015 / Accepted: 8 November 2015 / Published: 16 November 2015

Abstract: One of the main applications of field spectroscopy is the generation of spectral libraries of Earth's surfaces or materials to support mapping activities using imaging spectroscopy. To enhance the reliability of these libraries, spectral signature acquisition should be carried out following standard procedures and controlled experimental approaches. This paper presents a standard protocol for the creation of a spectral library for plant species. The protocol is based on characterizing the reflectance spectral response of different species in the spatiotemporal domain, by accounting for intra-species variation and inter-species similarity. A practical case study was conducted on the shrubland located in Doñana National Park (SW Spain). Spectral libraries of the five dominant shrub species were built (*Erica scoparia*, *Halimium halimifolium*, *Ulex australis*, *Rosmarinus officinalis*, and *Stauracanthus genistoides*). An estimation was made of the separability between species: on one hand, the Student's t-test evaluates significant intra-species variability ($p < 0.05$) and on the other hand, spectral similarity value (SSV) and spectral angle mapper (SAM) algorithms obtain significant separability values for dominant species, although it was not possible to discriminate the legume species *Ulex australis* and *Stauracanthus genistoides*.

Keywords: field spectroscopy; plant spectral library; standard protocol; Doñana National Park; shrublands

1. Introduction

In order to develop understanding of the effects of ecological processes and perturbations on the spatiotemporal distribution of plant communities, organizations responsible for managing protected natural areas require vegetation mapping at species level [1]. Furthermore, the ability to map and monitor changes in species composition over time optimizes management plans in these areas and is useful in tracking the spatiotemporal trends of invasive and keystone species [2].

Hyperspectral remote sensing has the potential to provide quantitative information on spatial cover, species composition, and the physicochemical status of vegetation, a capability that has already been demonstrated [3]. Among hyperspectral techniques, imaging spectroscopy is well developed on airborne platforms and has recently gained ground with the deployment of Unmanned Aerial Vehicles (UAV), although the process is still in its initial stages for spaceborne instruments [4]. In this respect, forthcoming space missions, such as EnMAP [5] or PRISMA [6], will bolster to move forward in the consolidation of hyperspectral techniques. Field spectroscopy predates the development of airborne or spaceborne imaging spectroscopy by many years [7], and has experienced remarkable growth over the past two decades in terms of its use and its application in different scientific disciplines.

Although imaging spectroscopy data looks promising for plant species mapping, few operational approaches exist because of our limited biophysical understanding of when remotely sensed signatures indicate the presence of unique species within and across plant communities [8]. Two of the main drawbacks in this respect are: high spectral similarity among species with similar ecological adaptations [9]; and, in contrast, high spectral variability response within species due to the variation ranges in plant constituents (such as tissue chemistry and structure) across environmental gradients [10]. Besides these drawbacks, vegetation phenology is layered on the top, a factor reducing inter-species similarity while at the same time increasing intra-species variation ranges [11].

In order to improve mapping efficiency using imaging spectroscopy, the analysis techniques applied to imagery could provide more satisfactory results by introducing ground-truth data to characterize the spectral response of every plant species studied [12]. However, field spectroscopy is the primary method used to collect ground-truth data for the development of reference spectral libraries [13]. In addition, a vast amount of literature documenting the potential of using plant spectral libraries for vegetation mapping is available (see Section 2). Nevertheless, in order to create consistently unique and detectable spectral signatures among species, spectral libraries should take into account the spatiotemporal variability of plant species across plant communities and throughout the seasons [14].

To ensure improvements in the reliability of these spectral libraries using imaging spectroscopy, reflectance spectral signature acquisition on field campaigns should be based on standard procedures and follow controlled experimental approaches [15]. Furthermore, the important constraints imposed by the complexity of natural illumination and huge variability in the components of a field spectroscopy campaign (*i.e.*, measurement sites, selected targets, sampling protocol), demand a complete metadata

system to properly report on what has been measured and the conditions in which the measurements were carried out [16].

At present, there is no standard harmonized protocol for the measurement of field reflectance in plants [17]. In this paper, we propose a complete methodology for the creation of a spectral library suitable for plant species mapping. This protocol seeks to establish standard procedures for the acquisition of plant spectra in the field, based on a number of solid bases for any plant type, but also including flexible procedures depending on the type of plant considered (*i.e.*, forest, shrub, pasture). One of these solid bases for the protocol is to estimate inter-species spectral similarity and intra-species variability by accounting for environmental gradients and phenological changes. To demonstrate the usability of the protocol, a practical case study was conducted in the shrub communities located in the stabilized sand dune ecosystem in Doñana National Park (SW, Spain).

2. Background: Current Status of Field Spectroscopy for Plant Spectral Library Generation

Before outlining the proposed protocol, this section notes several general issues in generating plant spectral libraries: it summarizes the current status of field spectroscopy in the solar spectrum; it highlights the most specific aspects of the acquisition of plant spectra in the field, and finally, it lists the most widely used spectral separability metrics.

2.1. Field Spectroscopy

Field spectroscopy is the measurement of high-resolution spectral radiance or irradiance in the field and is applied to retrieve the reflectance or emissivity spectral signatures of terrestrial surface targets. Compared with airborne or spaceborne imaging spectroscopy, the sensing instrument in the field can remain fixed over the subject of interest for much longer, thereby reducing the path length between the instrument and the object being measured [7].

The rugged and portable spectroradiometers currently available have evolved from the non-imaging spectrometers commonly used in the laboratory. Field spectroradiometer manufacturers fundamentally offer two types of instruments: (1) small, light devices that are designed to work only in the visible near infrared (VNIR: 350–1000 nm), with a signal-to-noise ratio (SNR) of around 250:1; (2) larger, heavier devices that are sensitive to the entire solar spectrum, with refrigerated shortwave infrared (SWIR: 1000–2500 nm) detectors and an SNR of around 1000:1. Depending on the application, these spectroradiometers can be configured for the sampling interval and spectral resolution. A typical configuration sets a full width at half maximum (FWHM) of nearly 3 nm in the VNIR spectral region, and about 10 nm in the SWIR region, although for more specific applications (*i.e.*, fluorescence measurements) a FWHM of 1 nm is required in the VNIR.

Spectral radiance measurement using the supplied fiber optic bundle with the option to attach different optics for Field Of View (FOV) variation has become widespread in recent years. Currently, field spectroscopy using hyperspectral imaging sensors or cameras is becoming increasingly relevant and is promising, although problems of scale and non-linear effects in this near-object imaging observation still need to be addressed [18]. The most widely used acquisition methodology to obtain near-ground reflectance is the *single-beam*, where the same instrument is used to measure both the target and the calibration panel spectral radiance. For these cases, the Spectralon® (Labsphere, North Sutton, NH,

USA) has become the standard material for the panels. Measurements are typically taken with field spectroradiometers that are hand-held, usually with the sensor head mounted on a pole or yoke to keep it away from the operator's body. For more automated remote observations UAVs are also being tested. Although challenging to use, they offer a high degree of automation and fast throughput [19]. In this regard, it is worth highlighting the novel carrier-lift system MUFSPeM@MED (Mobile Unit for Field SPeCttral Measurements at the MEDiterranean) [13], which provides extremely controlled measurements and is automatically operated from the ground.

Spectral libraries are collections of spectra that characterize the reflectance or emissivity spectral response of terrestrial surfaces and materials. Because spectral acquisition is largely variable, the simplest way to build a spectral library is by computing mean spectra and applying the standard deviation of the measured target to collect endmembers [16]. However, more complex cases can also include the spatiotemporal variation of a surface or material in order to characterize different properties or conditions (*i.e.*, different phenological stages in a plant spectral library [20]).

The existence of extensively documented metadata on spectral libraries enhances the suitability, long-term usability, and quality assurance of data from other researchers [21]. In Rashaid *et al.* [22] the most important field spectroscopy metadata was highlighted by advanced users, and Jimenez *et al.* [23] introduced an approach to establish a standard metadata system for field spectroscopy based on ISO and OGC standards.

2.2. Spectral Signature Acquisition

The spectral response of plants is a function of the optical properties of their constituents and structural attributes [10]. The chemical properties of pigments, water, and dry-matter content create distinct absorption features across the reflectance spectra. Because canopies have an intricate architecture, with gaps in the leaves and branches, the scattering and directional response may vary according to structural properties such as the Leaf Area Index (LAI) and Leaf Angle Distribution (LAD) [10]. The theoretical function describing the relationship between the incident flux and the distribution of what is reflected is referred to as the Bidirectional Reflectance Directional Function (BRDF) [24]. It is therefore, necessary to account for the geometry of observation when obtaining plant spectra in order to rigorously compare the acquired measurements under different illumination and observation conditions.

Spectral characterization of plant species is always problematic due to variations in biophysical properties, physiology, environmental parameters, and phenology [25]. Even so, it is important to highlight that a large number of remote-sensing vegetation-mapping studies have focused on the acquisition of field spectra over different vegetation types: grasslands [26,27]; shrublands [28,29], marshlands [30], forest [31,32], and sub-aquatic [33].

Recent works have addressed the generation of a spectral library of plant species using field spectroscopy. Zomer *et al.* [14] described field reflectance measurements in wetland vegetation in California, Texas, and Mississippi and the corresponding spectral library generation. Manakos *et al.* [13] presented the first steps on how to organize a spectral database for common Mediterranean land cover types. More recently, Nidamauri *et al.* [20] built spectral libraries for different crops taking into account their phenological stages. As an extremely helpful starting point, the SPECCHIO [34] project provides

an online spectral database where research groups within the remote sensing community can interchange plant spectral libraries.

2.3. Spectral Separability Metrics

By comparing plant spectral signatures between and within species and detecting differences and distances in their spectral shape and reflectance, we can estimate the uniqueness of the spectral response of individual plant species. The most widespread spectral analytical procedures (*i.e.*, spectral matching, discriminant analysis) could be applied to reflectance, by looking for subtle differences in the spectra, to the first derivative spectra, or to the continuum applied. Continuum-removal is a normalization technique, resulting in a curve with values from 0 to 1, which emphasizes the location and depth of individual absorption features [35].

An extremely high variation value in the spectral reflectance response between plant individuals of the same species has been reported [36]. Several physical and empirical-based methods have been proposed to quantify this intra-specific variability. Physical methods use radiative transfer codes, which calculate the spectral response of plants as a function of their constituents' content. Among the many different codes published, the canopy bidirectional reflectance model, known as SAIL (Scattering by Arbitrary Inclined Leaves), the more recent version SAILH, and the PROSPECT leaf optical model are the most widely used to study spectral and directional reflectance response of a plant canopy in relation to vegetation biophysical characteristics [37]. However, numerical simulations of these codes are based on actual values of measured biophysical parameters (*i.e.*, chlorophyll content, LAI) in the study area [10]. Meanwhile, empirical methods aim to estimate variation directly from the spectra collected in the field or laboratory for plant individuals measured with replicated levels of every relevant plant parameter [25].

Spectral similarity measurements between two species estimate the similarity of both the shape and amplitude reflectance curves in individual canopies. There are two categories of similarity measurement: stochastic and deterministic [38]. Depending on the considered spectrum region, we can calculate a separate, punctual measurement for every wavelength range, or a global measurement when the entire spectrum is used in the calculation. Deterministic measurements include the Spectral Angle Mapper (SAM) [39], the Euclidean Distance, and Cross-Correlation. Stochastic measurements make use of the inherent properties of sampled data as self-information and define certain spectral information criteria, such as divergence, probability, and entropy. Univariate and multivariate statistical techniques including parametric and non-parametric analysis of variance, canonical and discriminant analysis are widely used spectral separability metrics [11].

3. Plant Spectral Library Protocol

Figure 1 schematizes the proposed protocol for generating a plant spectral library and displays the two different parts. On one hand, a sampling protocol [40], which is a combination of a sampling strategy and observation procedure, includes every single aspect of field campaign preparation and spectral acquisition. On the other hand, the data processing protocol caters for the preparation of spectral files, spectral library creation, and spectral separability quantification between and within the plant species presented. In a parallel effort, the time invested in metadata collection is surpassed by its benefits in

reducing system bias and variability [17]. In this sense, the protocol emphasizes the most important metadata needed to describe the spectral library according to Rashaid *et al.* [22] and Jimenez *et al.* [23].

The spectral library sampling protocol has to be constrained in accordance with the ultimate goal of spectral measurement. In this work, the spectral library collection aims to support imaging spectroscopy analysis in plant mapping. Our protocol is based on an empirical approach in which field spectroscopy campaigns are designed to acquire the field spectra of plant species, by covering representative variations related to phenology and different environmental gradients. The collected spectral libraries will therefore characterize specific plant spectral signatures by identifying their uniqueness among species. Moreover, the sampling protocol proposes different technical aspects according to the type of vegetation considered: grass, shrub, or trees (underwater vegetation is not considered).

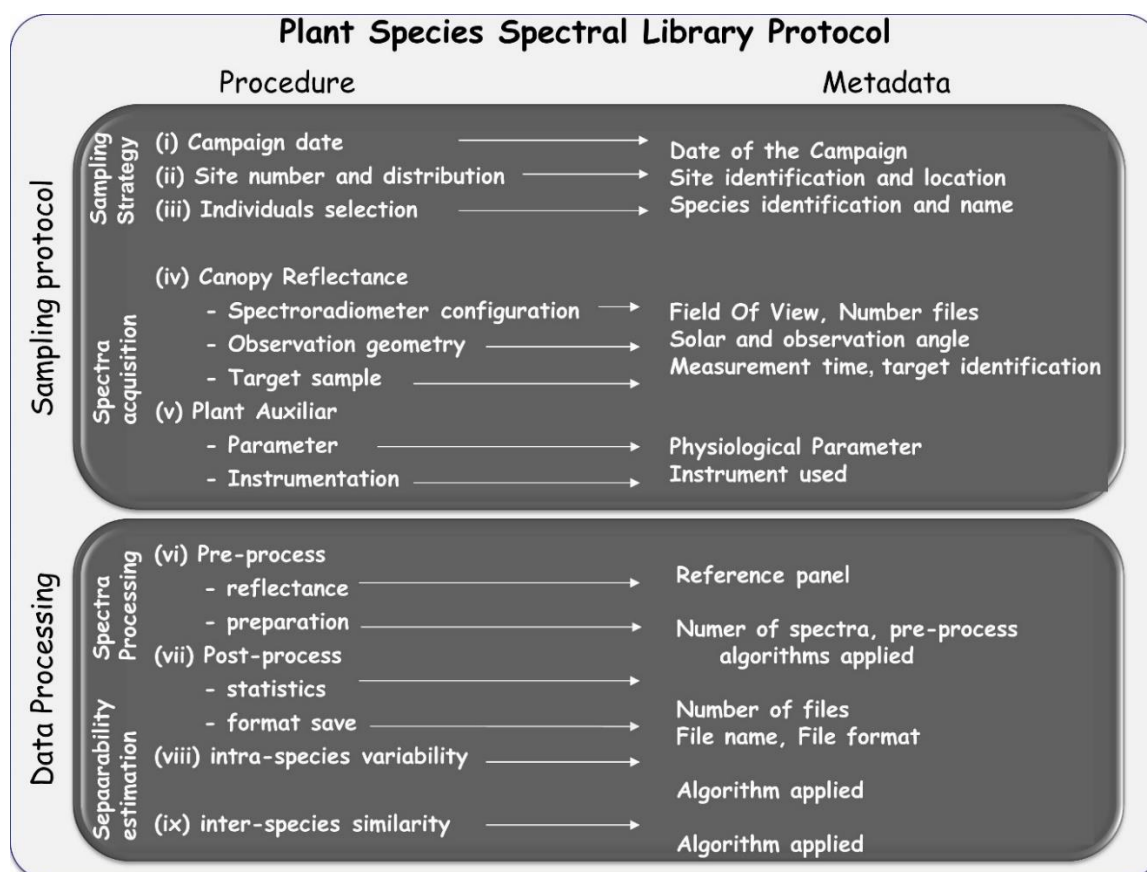


Figure 1. Field spectroscopy protocol for plant spectral library collection. The complete procedure and corresponding metadata are indicated for the sampling protocol and data processing.

3.1. Sampling Protocol

The sampling strategy designed should cover spatiotemporal variations for every species, taking into account the choice of the measurement sites and appropriate dates, and the selected sample individuals. The essential metadata for this section are location and identification of the measurement sites, as well as field campaign dates:

- (i) Field campaign dates should cover the phenological stages of the different species and identify seasonal differences in leaf aging, leaf drop, flowering and fruiting, and processes that affect relative proportions and the structural arrangement of chemicals exposed to the sensor over time. Depending on the plant community considered, two to four different dates throughout the year may be required to characterize spectral variation.
- (ii) The number of measurement sites and their spatial distribution has to cover the different plant communities presented, and should be stratified to account for environmental gradients (*i.e.*, soil type, topography). Stratified areas might be easily identified by using ancillary vegetation and topography maps of the study area, taking into account the extent of the area and its accessibility (*i.e.*, marshlands or very dense vegetation). The size of the measurement site is not relevant because the aim of the spectral library is the characterization of the species signature and endmember generation.
- (iii) The individuals to be measured may be selected by random sampling, but selected individuals should represent the “normal” state of the plant species and avoid damaged, sick, or juvenile individuals. The total number of individuals will be a function of the number of the definitive sampling sites, after the stratification process is completed. Several more individuals may be selected for plant communities with marked heterogeneity related to the environmental gradients observed. As an overall recommendation, at least 30 individuals are required for statistical reasons [41].

Acquisition of reflectance signatures in the field includes both the canopy reflectance and ancillary plant parameter measurements. The measurement technique for plant reflectance is based on spectral collection with a field spectroradiometer covering the whole plant canopy at the time of measurement. Reflectance measurements will represent the spatial assemblage of canopy constituents plus soil and understory plant elements, meaning that “contact probe” or laboratory measurements are not representative. Ancillary plant parameters may range from very simple information about plant status (*i.e.*, only record phenological stage) to measuring vegetation parameters with proper instrumentation (*i.e.*, pigment concentration or LAI). Metadata key elements for this section are: the spectroradiometer’s FOV applied, solar, and observation angles, measurement time, and ancillary plant parameters:

- (iv) In selecting and configuring the field spectroradiometer, the vegetation type must be considered. For instance, to accomplish lignin and cellulose absorption bands presented in woody species the field spectroradiometer should have sensing capabilities for the SWIR region [10]. For the appropriate determination of observation geometry, the instrument’s FOV should be broad enough to include every constituent of the canopy, capturing the entire size of tree canopies, shrubs or forbs by using poles, ladders, or cranes. However, the FOV should not be too large as to prevent signals from external elements around the measured plant. To select observation angles, nadir sampling is suggested in order to avoid hotspot effects. The whole canopy has to be sampled moving the spectroradiometer’s head within the canopy, recording various files per measurement to account for canopy variability. At this point, depending on the spectroradiometer used, attention must be paid to the actual pixel size with the fore-optic or fiber optic applied [42]. As recommended in general field spectroscopy protocols [43], the measurement time must be as close as possible to solar noon. For plant spectra acquisition, a field

spectroradiometer could be configured to acquire radiance or DN mode. After field spectroradiometer optimization, the radiance of the reference panel and plant canopy are registered. In order to minimize the variation in the output plant reflectance due to changes in solar illumination, the canopy and calibration panel radiance and sensor dark current should be measured nearly simultaneously.

- (v) The measurement of physicochemical parameters for the sampled individuals during spectral acquisition is strongly recommended. A vast amount of literature for this physiological parameter acquisition on site is available. For example, Jonckheere *et al.* [44] review several direct and indirect methods for LAI estimation. Methods for chlorophyll content or leaf water content measurements can be found in Gitelson [45] and Colombo *et al.* [46], respectively.

3.2. Data Processing and Spectral Separability Calculations

Spectra processing consists of pre-processing treatments to prepare reflectance readings for each canopy and post-processing procedures to record the data and metadata in standard format. Key metadata elements for this section are: file name, file size, applied algorithms, and selected output format:

- (vi) Field spectroradiometers usually have the option to register target and reference panel radiance measurements either jointly in the same file or in separate files. It is important to be aware that spectral data is usually saved in a proprietary format, which can only be read by specific software distributed by the manufacturer. Depending on the spectral noise level, polishing techniques, such as the Savitzky-Golay filter, might be applied but it is advisable to be conservative for the sake of preserving information [47]. In addition, it is also possible to apply spectral transformation (*i.e.*, continuum-removed, derivative). Similarly, all metadata on spectral acquisition should be addressed, by identifying the metadata source and data type: for example, recording information about the configuration of the spectroradiometer in the file, or saving a picture of the sampled plant species.
- (vii) During post-processing of spectra, the average reflectance and standard deviation are calculated for every measurement of the same target. To make data available for the scientific community, a common file format can be used: ASCII, Hierarchical Data File (HDF), jcamp-dx, or commercial imaging software format like the ENVI spectral library (Exelis Visual Information Solutions, Inc., Boulder, CO, USA). Similarly, metadata files should be generated and appended to the spectral library in a widely used and standard format. In this respect, Jimenez *et al.* [23] have suggested writing metadata files in Extensible Markup Language (XML) following international standards.

Once the canopy spectra for every individual has been measured, we can easily quantify spectral separability among species taking into account within-species variability due to physiochemical differences measured on site, and the similarity between species as well.

- (viii) Intra-species spectra variability may be checked based on the different phenological states and physiochemical parameters. The coefficient of variation (CV) or simple least square regression are statistical techniques that help to identify sensitive wavelength. In addition, univariate and multivariate statistical techniques, including both parametric and non-parametric analysis of

variance, can aid in the comparison of the spectral response over the different measurement dates in order to identify in which season the species easily discriminate from each other.

- (ix) The inter-species similarity index [11] can provide an estimation of differences in the spectral signature of plant species. In order not to lose possible subtle differences between species spectra, the protocol proposes the use of two different separability metrics for comparison, both applied either to the original and to the continuum-removed spectra.

4. Case Study: Shrublands of Doñana National Park

4.1. Study Area

Doñana National Park (DNP) is located on the southwest coast of Spain. It is one of the most important wetlands in Europe [48] and was designated a UNESCO World Heritage Site in 1995. DNP has a Mediterranean-type climate with some oceanic influences and mean annual precipitation of around 550 mm. Rainfall has a very well-defined seasonality, mostly concentrated between October and March (wet season) and almost absent between June and August (dry season). Three main land units have been traditionally distinguished in DNP: inland marshes, mobile sand dunes, and stabilized sand dunes. Our study was carried out in the stabilized sand dunes of the Doñana Biological Reserve (DBR), the core area of the DNP (Figure 2).

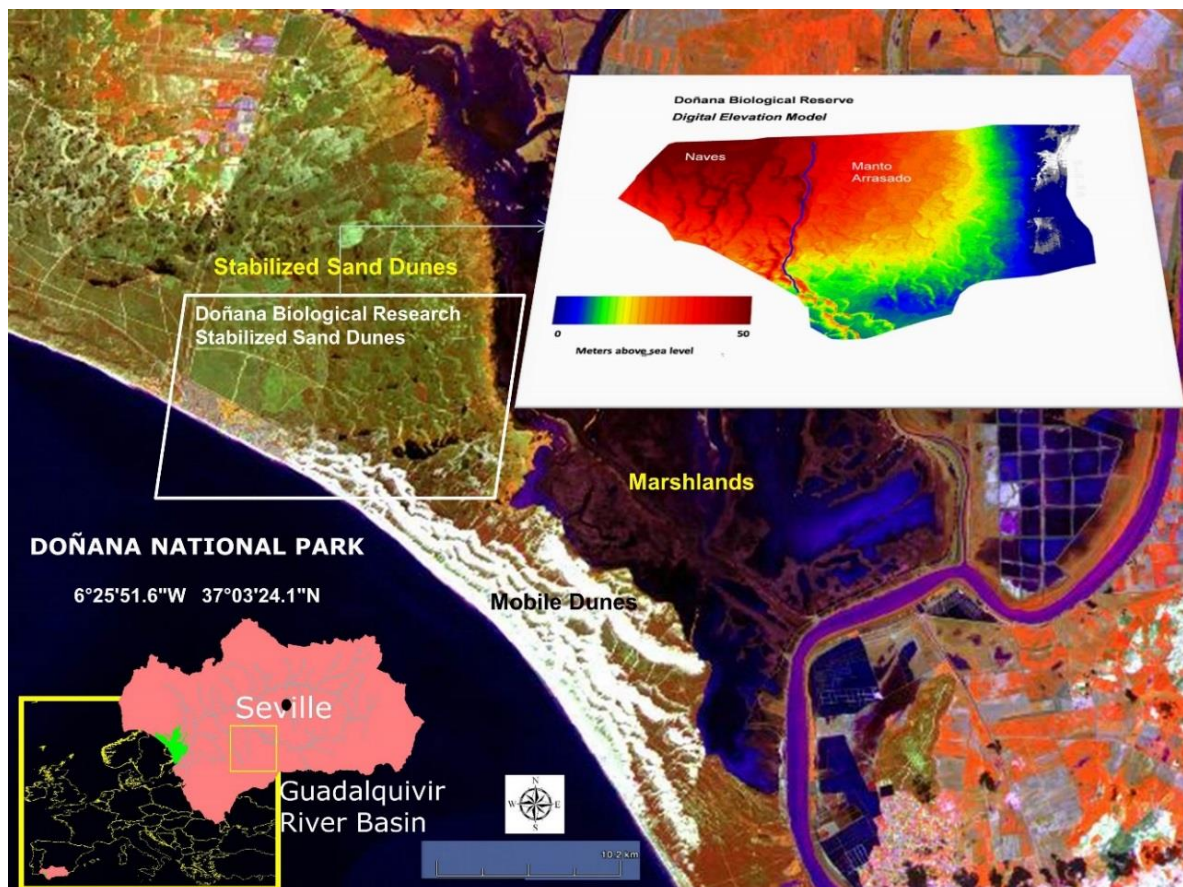


Figure 2. Location of Doñana National Park (SW, Spain). Square indicates the stabilized sand dunes ecosystem of Doñana Biological Reserve. The sub-image shows a digital elevation model of the study area.

Stabilized sand dunes exhibit a rolling topography (see Figure 2) due to the old dune morphology colonized by vegetation which is more or less dependent on groundwater supply. There are three large vegetation zones in the stabilized sand dunes of DBR: an elevated zone dominated by xerophytic shrubs (Naves), a lower zone dominated by hygrophytic shrub (Manto Arrasado), and the transitional grasslands (Vera). The current vegetation is composed of remnants of Mediterranean plant communities such as cork oak woodlands, juniper woodlands (*Juniperus phoenicea subs turbinata*), umbrella pine plantations (*Pinus pinea*), grasslands, and Mediterranean shrubland communities.






Three main types of shrub communities can be found on the stabilized sand dunes depending on the water table depth: Monte Blanco (Xerophytic sites), located on crests of former dunes where water table in summer is usually deeper than 4 m, and even over 3 m below the soil surface. This community is dominated by *Rosmarinus officinalis*, *Halimium commutatum*, *Halimium halimifolium*, *Juniperus phoenicea*, and *Cistus libanotis*. The Monte Negro (Hygrophytic sites) community is located at low depressions, where the water table in summer rarely lies 1 m below the soil surface and temporary ground flooding occurs in winter. This plant community is dominated by *Erica scoparia*, *Erica ciliaris*, *Calluna vulgaris*, *Ulex minor*, *Myrtus communis* and *Cistus salvifolius*. Finally, the Monte Intermedio community is located on the slopes of the dune ridges where the water table depth is in transition and there is no surface flooding. This community is dominated by *Halimium halimifolium* and *Ulex australis*. Spatial distribution of shrubland is determined, at all scales, by the rolling topography that modulates the groundwater level [49].

As for the structural characteristics of the studied shrub species, which may influence the canopy spectral response, three different leaf types were found: sclerophyll, semi-sclerophyll and spiny leaves [50]. Evergreen sclerophylls like, *E. scoparia*, are characterized by small, thick, leathery leaves, presenting a high surface-to-volume ratio. High leaf consistency and density is a trait that improves drought resistance in the Mediterranean summer climate [51]. These plants are isomorphic and their LAI values are constant throughout the year. Semi-sclerophyll species, also called xerophytic malacophylls, such as *H. halimifolium* and *R. officinalis*, have leaves with less density. Although they do not present foliar dimorphism, they may show important variations in LAI due to leaf substitution during summer. Spiny leaves developed by legume species *S. genistoides* and *U. australis* occupy the lower levels of LAI in Doñana's shrublands [52].

4.2. Shrub Species Spectral Library

Shrubland communities play an important role in DNP as a feeding and refuge habitat for local fauna. According to field studies conducted and available literature [49,50], five species are the most abundant and dominant across the stabilized sand dunes ecosystem: *Erica scoparia*, *Halimium halimifolium*, *Ulex australis*, *Rosmarinus officinalis*, *Stauracantus genistoides*. Table 1 shows several physiochemical characteristics of these dominant shrub species, the spectral library protocol was specially adapted to collect the reflectance signature of these shrubland species, taking into account their characteristics, such as plant height and canopy size. Furthermore, due to the LAI variations is a very important parameter in Mediterranean shrublands [50,51], *in situ* LAI measurements are acquired as ancillary information for the spectral library generation.

Table 1. Characteristics of the shrub dominant species in the stabilized sand dunes ecosystem of Doñana National Park.

Plant	<i>Erica scoparia</i>	<i>Halimium</i>	<i>Rosmarinus</i>	<i>Stauracanthus</i>	<i>Ulex australis</i>
Physiochemical Parameters		<i>halimifolium</i>	<i>officinalis</i>	<i>genistoides</i>	
					
Family	Ericaceae	Cistaceae	Lamiaceae	Leguminosae	Leguminosae
Common name	Brez de escobas	Jaguarzo blanco	Romero	Tojo Morisco	Tojo
Leaf type	Schlerophyll	Semi-Schlerophyll	Semi-Schlerophyll	spines	spines
Average Height	100 cm–3 m	60–150 cm	100–150 m	60–100 cm	60–100 cm
Canopy Diameter	1–2 m	50–100 cm	50–100 cm	50–100 cm	50–100 cm
Regeneration	roots	seeds	Seeds Horizontal	roots	roots
Root morphology	Horizontal	Horizontal/vertical	–11.0 Mpa	Horizontal/vertical	Horizontal/vertical
Leaf water potential	–3.0 Mpa	–4.0 Mpa		–1.7 Mpa	–2.7 Mpa

Below we follow the guidelines of the protocol (Section 3) to describe the procedures for generating the spectral library of the dominant shrub species in DNP:

- (i) To determine field campaign dates, we took into account the very sharp differences in water availability between the wet and dry seasons in DNP. Therefore, in 2006 and 2007, several field spectroscopy campaigns were carried out with measurements collected during the end of the dry season (late March and early April) and the end of the wet season (late August and early September). In the wet season campaigns, no measurements were taken during the flowering period of the Doñana shrubland, which takes place mainly between May and June.
- (ii) In the stabilized sand dune ecosystem, micro-topography is the major factor conditioning the sampling stratification. A 10 m pixel digital elevation model and the DBR Ecological Map were used for the stratification of the study area. To select sites along the stratified areas, locations for plant spectral acquisition and LAI measurements were determined using maps, but the choice was constrained by proximity to pathways due to the great difficulty of accessing areas with dense vegetation. A total of 16 measurement sites were selected, 12 of them intended for the acquisition of spectral signatures, while in the four other sites spectral signatures were acquired together with LAI measurements. Figure 3 shows sampling sites distribution, eight of those were located in the Naves, and the other eight sites in Manto Arrasado.
- (iii) Two types of canopy spectral measurements with two different aims were recorded: type (I) in order to generate spectral libraries for the five dominant species, 30 individuals for every dominant species were non-randomly selected covering the LAI ranges presented in the stabilized sand dune ecosystems. These measurements were carried out in spectral signature and LAI measurement sites (red tacks in Figure 3) and the individuals were marked and measured in wet and dry seasons; type (II) in order to calculate the spectral variability among the most abundant shrub species, canopy spectral reflectance was also measured for the five dominant species and other abundant shrub species (*Lavandula stoechas*, *Thymus mastichina*,

Cistus libanotis, *Halimium commutatum*, *Phylirrea angustifolia*). These measurements were carried out in spectral signature sites (yellow tacks in Figure 3) only in the dry season and for 30 randomly selected individuals in every species; damaged or individuals in early growing stages were avoided.

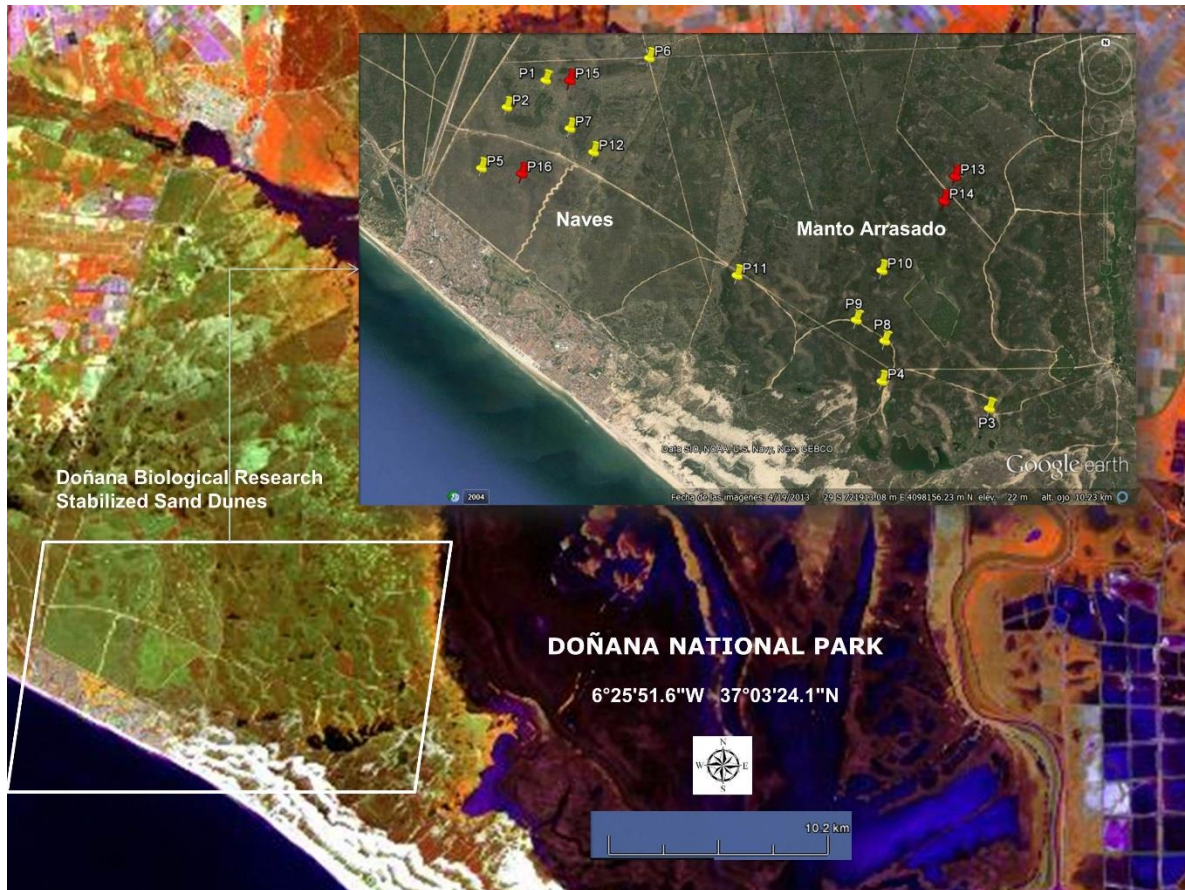


Figure 3. Site location for plant spectral library measurements. Yellow tacks identify spectral signatures acquisition sites and red tacks identify spectral signatures and LAI measurements sites.

- (iv) Shrub species have a considerable woody part, which recommended the use of a spectroradiometer with a SWIR detector. The field spectroradiometer chosen was the ASD FieldSpec3 (Analytical Spectral Devices, Boulder, CO, USA), which measures incoming radiance using a fiber optic which is adaptable with a fore optic lens. It has a spectral range from 350 to 2500 nm with a 3 nm spectral resolution and a sampling interval of 1.4 nm in the VNIR spectral regions and 10 nm and 2 nm in the SWIR. Measurements were acquired directly with the fiber optic (FOV 25 °) with no fore-optics mounted. The fiber was nadir-oriented and held 1 m above the canopy (GIFOV = 44 cm). For tall individuals a leader was used to maintain a constant distance between the fiber and canopy. Target and reference panel radiance were alternatively acquired and the instrument's dark current was measured before each sampling. At least five files per plant, averaging five spectra per file, were recorded on a whole sweep of the canopy. During sweeping the pistol grip was continuously turned clockwise and counter-clockwise to minimize spectral misalignments of the ASD fiber [42].

Measurements were concentrated in two hours around noon. The field campaigns were always carried out under cloudless skies.

- (v) LAI measurements were carried out in some individuals at the same time as the reflectance spectral acquisitions. We used an indirect method and took hemispherical canopy pictures for each plant. These 180 ° pictures were always taken from beneath the canopy looking upwards with a NIKON FC-E8 fisheye lens adapted to a Nikon 4000 Coolpix digital camera. The pictures were always gathered at nearly sunset [53]. In this process, the Plant Area Index (PAI) which also includes non-photosynthetic elements, such as branches, was estimated instead of the LAI. The PAI was calculated by processing the corresponding hemispherical canopy picture with Hemiview® 2.1 (Delta-T Devices, Ltd., Cambridge, UK). This software estimates gap fraction over the entire picture and calculates the PAI. In Figure 3, the sites for the PAI measurements are indicated with red tacks.
- (vi) Spectral files acquired using ASD Fieldspec3 were imported to ASCII format using ViewSpec® software. Canopy reflectance per plant (five measurements) was calculated by dividing target and reference panel radiance. All collected spectra were parabolic-corrected for the spectroradiometer sensitivity drift at the junctions of the spectral regions of the three different detectors. No spectral polishing algorithm was applied.
- (vii) For each plant individual, an average reflectance spectral signature and standard deviation (SD) file was generated. Spectral reflectance at wavelengths of around 1400 nm, 1940 nm, and 2400 nm were excluded due to the presence of excessive noise caused by atmospheric water absorption. The output file was saved in the ENVI spectral library format (Exelis Visual Information Solutions, Inc., Boulder, CO, USA).
- (viii) Once the canopy reflectance spectra for every plant individual was calculated, the spectral library for the five dominant species were generated using the spectra from Type-I measurements. The species coefficient of variation (CV) in dry season was calculated using the spectra for which PAI was measured. CV was calculated for every wavelength and an averaged value was calculated for the entire spectral region. To determine the season when dominant species show greatest variability and most differences between each other, parametrical statistical tests were applied to compare species of Type-I measurement per season. A standard series of two-group t-tests were performed for every wavelength to test the null hypothesis that there were no significant differences between means. This test allows for the identification of the wavelength region where the species show higher spectral separability. Normality was previously explored and confirmed with the Kolmogorov–Smirnov normality test.
- (ix) Similarity indexes between species were calculated. In this case, global similarity methodologies were applied on Type-II measurements. Two deterministic algorithms were calculated using the original and continuum-removal algorithm applied to entire spectra. These two algorithms were the Spectral Similarity Value (SSV) [54] and SAM. SSV takes into account curve shapes by comparing correlation and separation calculated by Euclidean distance. By definition, the spectral similarity scale has a minimum of 0 and a maximum of the square root of 2. Low values in the similarity scale indicate similar spectra. SAM calculates the angular distance between two reflectance vectors across wavelengths, and is less sensitive to the

amplitude of both spectra. Range values vary from 0 to $\pi/2$, where a lower SAM angle means a higher similarity between two spectra.

5. Results

The main outcome of our work are the spectral libraries for the five dominant shrub species in DNP; they provide significant support to vegetation mapping using airborne imaging spectroscopy (reported in Jiménez *et al.* [55]). However, intra-species variability between dominant species is also conveyed which contributes to determining the suitable season and spectral region for mapping activities. We also report differences between the five dominant shrub species and other less abundant species present in the study area.

5.1. Dominant Species Spectral Library

Figure 4 shows an average spectral signature for the five dominant species of Doñana's shrublands. The spectral library curves for the dry and wet season show the mean and SD across the measured PAI gradient found in the stabilized sand dunes plant communities. Figure 4 also shows the averaged PAI values and corresponding CV calculated for every species during dry season. Although *R. officinalis* exhibits the highest CV, the greater PAI range was found for *H. halimifolium*, meaning that PAI changes have a greater influence on the spectral response of *R. officinalis*. The lowest CV values and the lowest PAI spectral response variations were found in both legume species *S. genistoides* and *U. australis*.

A visual examination of the spectral library graphics (see Figure 4) highlights the similarity between species, as might be expected for a group of species growing in a very similar environment with very similar conditions (poor soils, high radiations levels, and long drought periods). Focusing on the five dominant species for both seasons, distinct absorption features in their spectral signatures may be related to their structural arrangement. For green leaves, chlorophyll a and b and accessory pigments (*i.e.*, carotenoids) dominate absorption features in the visible spectrum (400–700 nm). Water creates absorption features in the near-infrared at 970 nm and 1188 nm, respectively. However, in the shortwave infrared, relatively low reflectance values and strong water absorption regions are found in green leaves.

When comparing the spectral signatures between seasons, subtle differences are revealed, such as lower variability (lower SD) values for all the species in the wet season, and deeper NIR water absorption bands, which almost disappear in legume species in the dry season. The most evident differences are noticeable for lignin and cellulose absorption bands, centered at 2100 and 2310 nm, which are deeper in dry season spectra for all species. This is because those bands are masked in wet season due to the higher water content. Muddle differences are found in the reflectance response between species: on one hand, we found higher reflectance in the VIS part for dry season spectra, mostly due to a lower concentration of leaf pigments; on the other hand, lower reflectance in the NIR part, except for *E. scoparia*, due to a higher structural arrangement of tissues in crowns, measured through leaf and branch density, angular distribution, and clumping [45].

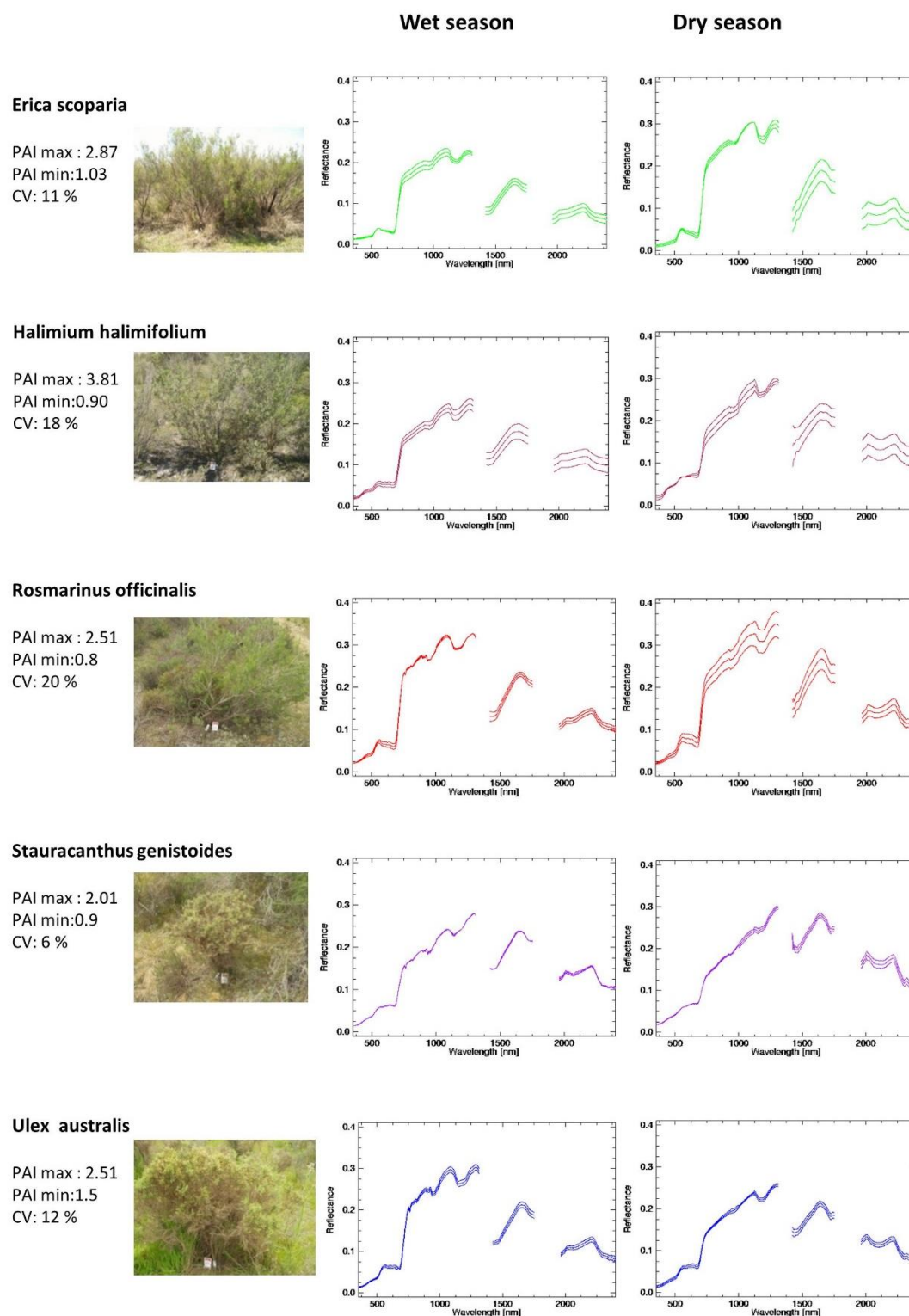


Figure 4. Spectral library of the five dominant shrub species in Doñana National Park. The graphics show the average and standard deviation spectral reflectance for dry and wet season. PAI and CV values are shown for every species spectral response in dry season.

5.2. Intra-Species Variability

The standard t-test evaluates if the intra-species variability was significantly different between species. The means of two species were considered significantly different when calculated t-values were

greater than the t-critical value ($p < 0.05$). The t-value was calculated assuming pooled variance (rather than separate variances), because the number of spectral samples was different for each species and their variances were unequal/no-paired (F-test). Single graphics in Figure 5 show every two-species comparison, where the curve represents the calculated t-value per wavelength. The red line in the graphics identifies t-critical values corresponding with the degrees of freedom in the sample.

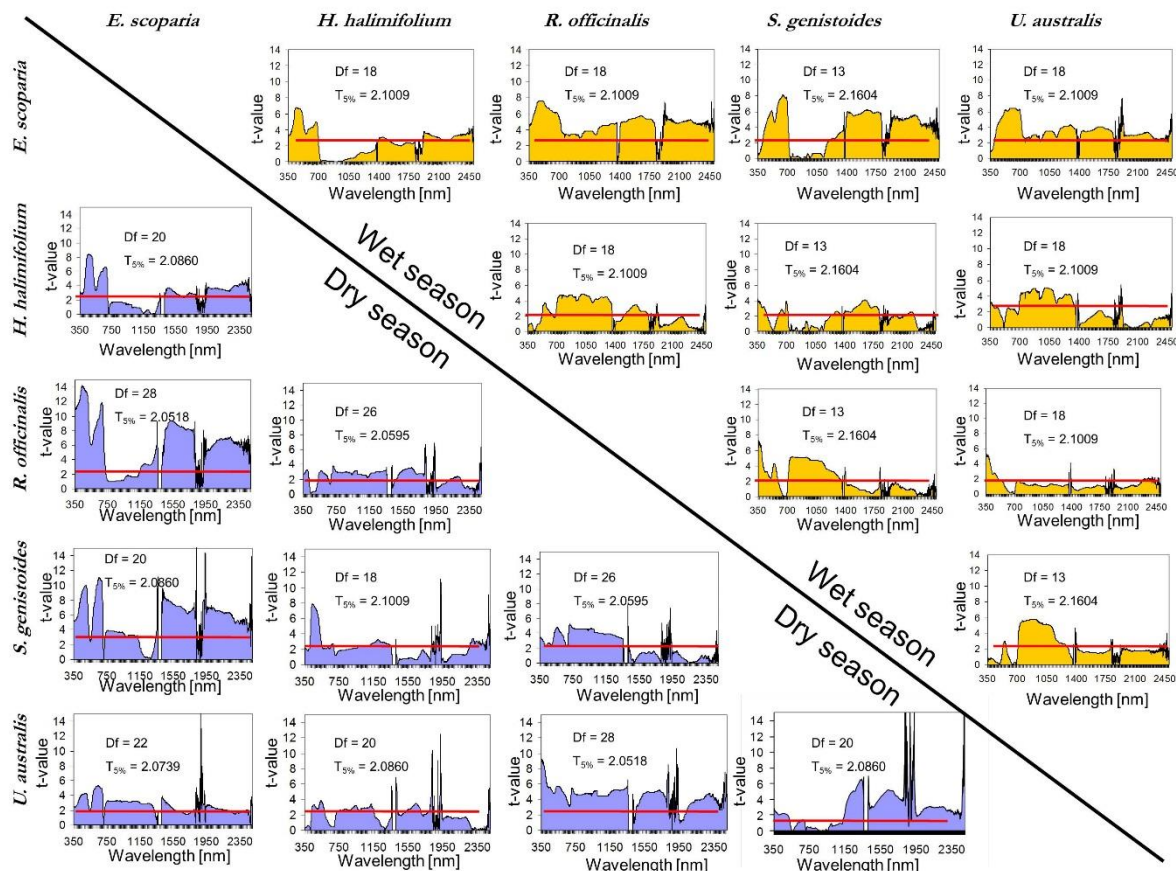


Figure 5. Intra-species variability for the DNP shrubland dominant species. t-test for species-to-species comparison for dry and wet season separately. The red line in the graphics identifies t-critical values according to the corresponding degrees of freedom.

According to Figure 5, dry season measurements show a slightly higher discrimination power among species than those collected during wet season. Although in dry season the species show more variable signatures (see Figure 4), they are also more different among themselves and its variability is less significant. For example, in the VIS part of the spectrum five species during dry season, and *E. scoparia* has higher calculated t-values in the dry season than in the wet season.

It is evident that some bands have more power for discriminating between species, since they have a higher frequency of statistically different mean reflectance. The tests were calculated independently for each wavelength value. We therefore used this local similarity algorithm to locate the spectral regions where the differences were systematically higher. For the dominant shrub species the best spectral regions to discriminate between species ($p < 0.05$), were found at (480, 690, 770, 979, 1600, and 2100 nm) both during the dry and wet seasons.

5.3. Inter-Species Similarity

Spectral reflectance similarity indexes were calculated among the dominant shrub species and also for less abundant species present in the Doñana shrubland communities. Figure 6 presents similarity indexes between all the shrub species studied and were calculated using SSV and SAM algorithms, by comparing both the original and the continuum-removed applied spectra. The highest dissimilarity values identified, and represented in white, were 0.4 for SSV and 0.6 for SAM. In Figure 6, shrub species name were underlined according to Doñana's shrubland community. Furthermore, to assess the importance of foliage type in the spectral signature and its discriminability, shrub species names were colored according to foliage type.

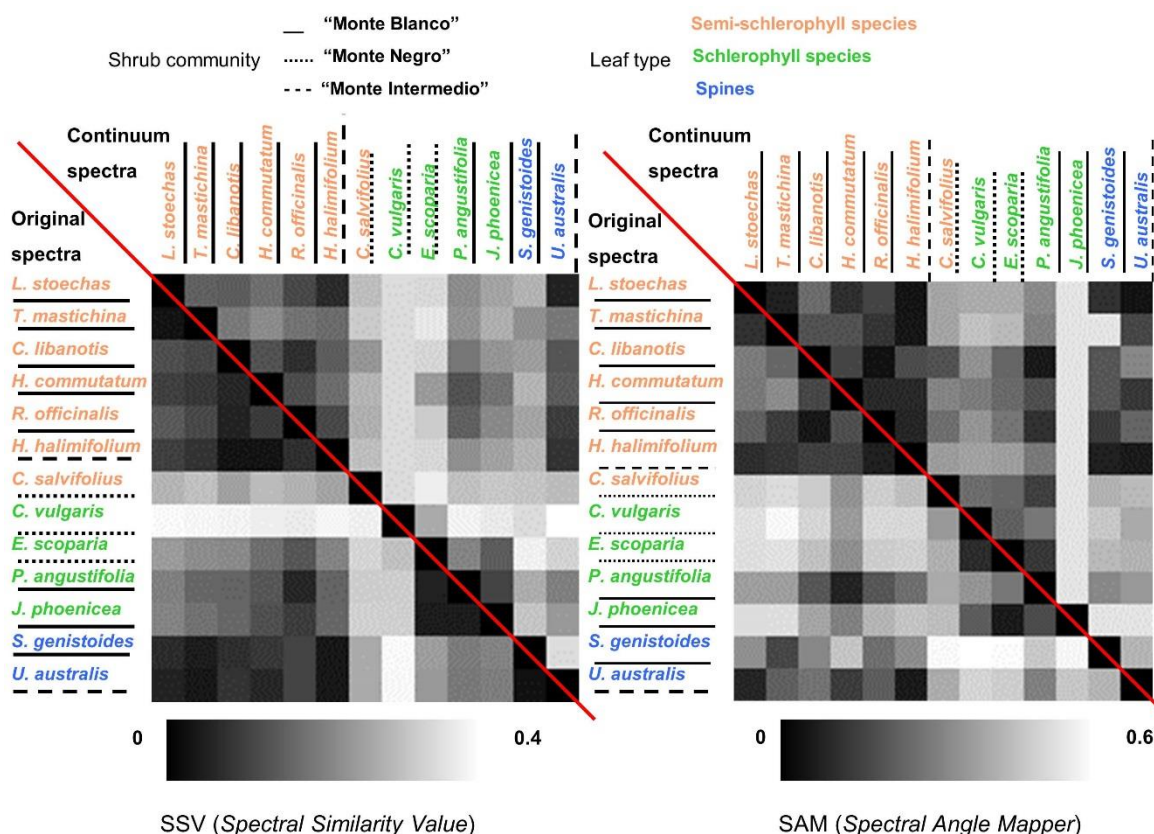


Figure 6. Matrix of spectral similarity indexes in grayscale, where black indicates total similarity and white the highest dissimilarity for the dominant and the less abundant shrub species in Doñana National Park. Foliage type is also shown by coloring the species name. Species names are also underlined according to the shrubland community they belong to.

5.3.1. Leaf Type Comparison: within and between Leaf Type Groups

Semi-schlerophyll species showed intermediate similarity values, with values of less than 0.2 for both algorithms and spectral signature process type. For this leaf type, continuum-removed spectra had higher SSV values than the SAM algorithm. Furthermore, *C. salvifolius* reached the higher values of dissimilarity, 0.3 for SSV and 0.4 for SAM, when compared to the other semi-schlerophyll species. Schlerophyll species presented smaller dissimilarity values, for both algorithms and spectral signature process type, than the rest of the leaf types. In this case, the SSV algorithm showed higher values than

SAM, meaning a greater separability capacity. Finally, spiny legume species also showed intermediate values of similarity. The SAM algorithm produced the best separation.

When comparing semi-schlerophyll and schlerophyll species, considerable dissimilarity values for both algorithms were found (SSV = 0.3, SAM = 0.5). In this case, the SAM algorithm from the original spectra produced a slightly better separability. Spiny legume species were found to be much more dissimilar to schlerophyll species than to semi-schlerophyll species for both algorithms, reaching values of around 0.25 for SSV and 0.35 for the SAM. In this case, the SAM calculated from the original spectra yielded slightly higher dissimilarity values for both leaf types; *S. genistoides* was the spiny legume species with higher separability values than the schlerophyll species.

5.3.2. Within and between-Communities Species Comparison

Monte Intermedio species showed the lowest dissimilarity values for the species within it (SSV = 0.15, SAM = 0.25). Although *H. halimifolium* is a semi-schlerophyll species and *U. australis* is a spiny legume species, it had lower dissimilarity values than expected for species of different plant communities. In contrast, higher separability values were found within the Monte Negro species. In this case, even the comparison between two schlerophyll species *E. scoparia* and *C. vulgaris* provided high separability values, and showed the highest differences with *C. salvifolius*. Monte Blanco showed different levels of dissimilarity, with intermediate values (SSV = 0.2 and SAM = 0.3) within semi-schlerophyll species, and higher values between schlerophyll species *P. angustifolia* and *J. phoenicia* in comparison to other semi-schlerophyll species and the spiny legume *S. genistoides*.

In the comparison between species of different communities, all three communities presented very separable values among each other. The highest dissimilarity values were found for Monte Negro compared with the other two communities. SAM produced the highest differences (SAM = 0.5 and SSV = 0.35). Dissimilarity values decreased when comparing Monte Blanco species with Monte Intermedio. Again, SAM was found to provide the highest differences between communities.

5.3.3. Comparison within Dominant Species

Considering dissimilarity values between the dominant species, *E. scoparia* had the highest values compared with the other species. In this comparison, SAM from original spectra showed the best performance. Other high separability values were found for the spiny legume *S. genistoides* when compared to the schlerophyll *E. scoparia*. Furthermore, between the two spiny legume species the separability values were intermediate and acceptable to discriminate them. In contrast, the lowest dissimilarity values were found between the spiny legume *U. australis* and the semi-schlerophyll *H. halimifolium*. Although separability values between these two Monte Negro community species were lower, the discrimination power is still suitable for mapping activities. Finally, the semi-schlerophyll species *H. halimifolium* and *R. officinalis* showed intermediate separability values.

6. Discussion

In this work, we proposed a protocol for developing a plant spectral library focusing on its application in supporting mapping activities with imaging spectroscopy. The proposal aims to ensure standard and

highly repeatable measurements. Nevertheless, it also has to be flexible enough to adapt the procedures (*i.e.*, field spectroradiometer, observation geometry, number of dates, and individuals) to vegetation type, to species diversity, and to the environmental heterogeneity of the study area.

One of the main drawbacks of the protocol is that plant spectral signatures were acquired over the entire canopy, including the spectral response to the background structural arrangements and understory vegetation. The principal argument underpinning this approach is that the plant spectral signature will support future analysis of airborne or satellite imaging spectroscopy, which captures the whole canopy signal plus background spectral response in its pixels. Therefore, this field-level spectral signature is designed to integrate the at-sensor-level signal. For example, in Manevski *et al.* [29], the soil background from the acquired canopy spectra was treated as integrated parts of the vegetation spectra in typical Mediterranean semi-arid environments.

Another tricky point of the protocol is the procedure to estimate plant separability. We believe that the spectral library generation should evaluate the spectral variation throughout space and time, which means that intra-species variation is crucial *a priori* information to decide the optimum image acquisition date and to choose the best bands for species discrimination. Consequently, inter-species similarity quantification is secondary for the protocol, but very important to be able to estimate the degree of uniqueness of the species studied. In this sense, several methods of similarity metrics are widely available, as we pointed out in section 2.3. We recommend applying at least two different algorithms not just to the original spectral signatures, according to the possible, subtle differences between plant species.

In fact, the protocol was designed to be applied to different types of vegetation (*i.e.*, grasslands, shrublands, marshlands, forest), with the exception of sub-aquatic vegetation which implies more specific technical aspects for spectral signature acquisition. For other vegetation types, the sampling protocol should be adapted mainly in terms of the observation geometry.

The application of the protocol to Doñana's shrublands communities allows refinement of the methodology. The case study presented in this work was developed for a plant community with around 20 shrub species, where five are dominant. The majority of these shrub species, including dominant species, have canopy sizes of between two or three meters, and no more than three meters in height. The determinant environmental gradients for spatial patterns in species distribution (*i.e.*, micro-topography and ocean proximity) were addressed with the stratification sampling strategy. In any case, the Doñana shrubland spectral library is a typical mapping activity case, while in other complex cases of species diversity and characteristics, and environmental gradients, the protocol might be more challenging in terms of sampling strategy and spectra acquisition. However, in this case the most relevant constraint was the high plant density found for some areas of the Monte Negro shrubland.

In terms of the Doñana shrubland spectral libraries, the dominant species showed typical shrub spectra with differences enhanced according to the season in which the measurement took place. During the dry season, reduced water content in the leaves is revealed by low reflectance in the NIR and SWIR regions, while lignin and cellulose bands were more pronounced. Groundwater availability due to the ancient dune micro-topography is a major factor in the establishment and growth of plants; as a result, considerable PAI ranges were found for the dominant shrub species, especially for the more widespread *H. halimifolium*. Although significant spectral variation in shrubs in terms of PAI changes was found for

the spectral amplitude (SSV) but not in the shape (SAM), larger-amplitude spectral variability reinforces the need for empirical estimation of the spectral changes due to local environmental gradients in the area.

T-test evidenced that during the dry season the analyzed species had better separability than in the wet season. During drought conditions, the stabilized sand dune ecosystem shows a more homogeneous background with most of the underbrush vegetation being in a senescent stage. The spectral regions found with higher separability significance are usually related to plant water content (*i.e.*, water absorption bands) and indirectly to pigments, lignin, and cellulose contents.

The application of the protocol to other, less abundant species helped to identify discrimination features suitable to enhance mapping with imaging spectroscopy. Plant species discrimination is a very challenging application, even more so for species of the same vegetation type and living in similar environmental conditions. The use of different separation algorithms on both the original and continuum-removed spectra is strongly recommended in order to increase species separability.

7. Conclusions

This paper presents an approach to a standard protocol for spectral library generation to support vegetation mapping using imaging spectroscopy. The proposed protocol is based on field spectroscopy measurements to characterize the reflectance spectral response of the distinct species throughout spatiotemporal changes. To this end, we carried out several field campaigns in different seasons, following a stratified sampling strategy, taking into account the phenological stages and different spectral responses due to environmental gradients present in the study area. In addition, measurement of ancillary vegetation parameters together with spectral reflectance contributed to the empirical identification of spectral variability linked to environmental conditions. After the spectral libraries were collected, the separability between species was quantified by considering intra-species variability and inter-species similarity. Endmembers obtained from the spectral libraries were used as the main input for vegetation mapping with imaging spectroscopy of Doñana shrubland communities [55].

Overall, the analyzed species appeared very similar in spectral terms, as expected for a group of species living in an environment with very similar conditions, poor soils, high insolation, and low water availability. Nevertheless, separability indexes and PAI values calculated for the dominant shrub species were statistically significant, although Monte Negro species were the most difficult to discriminate. The spectral libraries built were used for planning the airborne imaging spectroscopy mapping campaigns in the Doñana National Park shrublands [55].

Acknowledgments

The authors are extremely grateful to the staff of the INTA Remote Sensing Laboratory for their scientific support and the staff of the Doñana Biological Research Station for their outstanding logistical support received in the course of the work. We appreciate the contribution of Antonio Pou, who largely supervised this work. We also thank Patrick Vaughan and Angela de Santis for field assistance in collecting PAI field measurements.

Author Contributions

Both authors are intellectually responsible for the research conducted. Marcos Jiménez designed the work presented and prepared the manuscript. Ricardo Dáz-Delgado was substantially involved in field spectroscopy acquisition and in reviewing the manuscript.

Conflicts of Interest

The authors declare no conflict of interest.

References

1. Schmeller, D.S. European species and habitat monitoring: where are we now? *Biodivers. Conserv.* **2008**, *17*, 3321–3326.
2. He, K.S.; Rocchini, D.; Neteler, M.; Nagendra, H. Benefits of hyperspectral remote sensing for tracking plant invasions. *Divers. Distrib.* **2011**, *17*, 381–392.
3. Ustin, S.; Zarco Tejada, P.; Jacquemoud, S.; Asner, G. Remote sensing of environment: State of the science and new directions. In *Remote Sensing for Natural Resources Management and Environmental Monitoring. Manual of Remote Sensing*, 3rd ed.; Ustin, S.L., Ed.; John Wiley & Sons, Inc.: Hoboken, NJ, USA, 2004; Volume 4, pp. 679–729.
4. Schaepman, M.E.; Ustin, S.L.; Plaza, A.J.; Painter, T.H.; Verrelst, J.; Liang, S. Earth system science related imaging spectroscopy—An assessment. *Remote Sens. Environ.* **2009**, *113*, 123–137.
5. Kaufmann, H.; Segl, K.; Kuester, T.; Rogass, C.; Foerster, S.; Wulf, H.; Hofer, S.; Sang, B.; Storch, T.; Mueller, A.; *et al.* The Environmental Mapping and Analysis Program (EnMAP)—Present status of preparatory phase. In Proceedings of the International Geoscience and Remote Sensing Symposium (IGARSS'13), Melbourne, Australia, 21–26 July 2013.
6. Romano, F.; Santini, F.; Simoniello, T.; Ananasso, C.; Corsini, G.; Cuomo, V. The PRISMA hyperspectral mission: Science activities and opportunities for agriculture and land monitoring. In Proceedings of the International Geoscience and Remote Sensing Symposium (IGARSS'13), Melbourne, Australia, 21–26 July 2013.
7. Milton, E.J.; Schaepman, M.E.; Anderson, K.; Kneubühler, M.; Fox, N. Progress in field spectroscopy. *Remote Sens. Environ.* **2009**, *113*, 92–109.
8. Asner, G.P.; Jones, M.O.; Martin, R.E.; Knapp, D.E.; Hughes, R.F. Remote sensing of native and invasive species in Hawaiian rainforests. *Remote Sens. Environ.* **2008**, *112*, 1912–1926.
9. Lewis, M.M. A strategy for mapping arid vegetation associations with hyperspectral imagery. In Proceedings of Eleventh Australian Remote Sensing and Photogrammetry Conference, Brisbane, Australia, 2–6 September 2002; pp. 647–655.
10. Asner, G.P. Biophysical and biochemical sources of variability in canopy reflectance. *Remote Sens. Environ.* **1998**, *64*, 234–253.
11. Clark, M.L.; Roberts, D.A. Species-level differences in hyperspectral metrics among tropical rainforest trees as determined by a tree-based classifier. *Remote Sens.* **2012**, *4*, 1820–1855.

12. Warner, T.A. Remote sensing analysis: From project design to implementation. In *Manual of Geospatial Sciences*, 2nd ed.; Bossler, J.D., McMaster, R.B., Rizos, C., Campbell, J.B., Eds.; Taylor and Francis: London, UK, 2010; Chapter 17, pp. 301–318.
13. Manakos, I.; Manevski, K.; Petropoulos, G.P.; Elhag, M.; Kalaitzidis, C. Development of a spectral library for Mediterranean land cover types. In *Proceedings of 30th EARSeL Symp.: Remote Sensing for Science, Education and Natural and Cultural Heritage*, Paris, France, 31 May–3 June 2010; pp. 663–668.
14. Zomer, R.J.; Trabucco, A.; Ustin, S.L. Building spectral libraries from wetlands land cover classification and hyperspectral remote sensing. *J. Environ. Manag.* **2008**, *90*, 2170–2177.
15. Ruby, J.G.; Fischer, R.L. Spectral signatures database for remote sensing applications. *Proc. SPIE* **2002**, *4816*, 156–163.
16. Hueni, A.; Malthus, T.; Kneubuehler, M.; Schaepman, M. Data exchange between distributed spectral databases. *Comput. Geosci.* **2011**, *37*, 861–873.
17. Pfitzner, K.; Bollhöfer, A.; Esparon, A.; Bartolo, B.; Staben, G. Standardized spectra (400–2500 nm) and associated metadata: An example from northern tropical Australia. In *Proceedings of IEEE International Geoscience and Remote Sensing Symposium*, Honolulu, Hawaii, USA, 25–30 July 2010.
18. Buddenbaum, H.; Stern, O.; Stellmes, M.; Stoffels, J.; Pueschel, P.; Hill, J.; Werner, W. Field Imaging spectroscopy of beech seedlings under dryness stress. *Remote Sens.* **2012**, *4*, 3721–3740.
19. Hruska, R.; Mitchell, J.; Anderson, M.; Glenn, N.F. Radiometric and geometric analysis of hyperspectral imagery acquired from an unmanned aerial vehicle. *Remote Sens.* **2012**, *4*, 2736–2752.
20. Nidamanuri, R.R.; Zbell, B. Use of field reflectance data for crop mapping using airborne hyperspectral image. *ISPRS J. Photogramm. Remote Sens.* **2011**, *66*, 683–691.
21. Hueni, A.; Nieke, J.; Schopfer, J.; Kneubuehler, M.; Itten, K.I. The spectral database SPECCHIO for improved long-term usability and datasharing. *Comput. Geosci.* **2009**, *35*, 557–565.
22. Rasaiyah, B.; Jones, S.; Bellman, C.; Malthus, T.J. Critical metadata for spectroscopy field campaigns. *Remote Sens.* **2014**, *6*, 3662–3680.
23. Jiménez, M.; González, M.; Amaro, A.; Fernández-Renau, A. Field spectroscopy metadata system based on ISO and OGC standards. *ISPRS Int. J. Geo-Inf.* **2014**, *3*, 1003–1022.
24. Nicodemus, F.E.; Richmond, J.C.; Hsia, J.J.; Ginsberg, I.W.; Limperis, T. *Geometrical Considerations and Nomenclature for Reflectance*; National Bureau of Standards, US Department of Commerce: Washington, DC, USA, 1977.
25. Thenkabail, P.; Lyon, J.; Huete, A. Advances in hyperspectral remote sensing of vegetation and agricultural croplands. In *Hyperspectral Remote Sensing of Vegetation*; Thenkabail, P.S., Lyon, J.G., Huete, A., Eds.; CRC Press/Taylor and Francis Group: Boca Raton, FL, USA, 2011; pp. 3–36.
26. Miao, X. Estimation of yellow starthistle abundance through CASI-2 hyperspectral imagery linear spectral mixture models. *Remote Sens. Environ.* **2006**, *101*, 329–341.
27. Möckel, T.; Dalmayne, J.; Prentice, H.C.; Eklundh, L.; Purschke, O.; Schmidtlein, S.; Hall, K. Classification of grassland successional stages using airborne hyperspectral imagery. *Remote Sens.* **2014**, *6*, 7732–7761.
28. Roberts, D.A.; Gardner, M.; Church, R.; Ustin, S.; Scheer, G.; Green, R.O. Mapping chaparral in the Santa Monica mountains using multiple endmember spectral mixture models. *Remote Sens. Environ.* **1998**, *65*, 267–279.

29. Manevski K.; Manakosa, I.; Petropoulos, P.; Kalaitzidis, C. Discrimination of common Mediterranean plant species using field spectroradiometry. *Int. J. Appl. Earth Obs. Geoinf.* **2011**, *13*, 922–933.
30. Silvestry, S.; Marani, M.; Marani, A. Hyperspectral remote sensing of salt marsh vegetation. *Phys. Chem. Earth.* **2003**, *28*, 15–25.
31. Kalacska, M. Ecological fingerprinting of ecosystem succession: Estimating secondary tropical dry forest structure and diversity using imaging Spectroscopy. *Remote Sens. Environ.* **2007**, *108*, 82–96.
32. Somers, B.; Asner, G.P. Hyperspectral time series analysis of native and invasive species in Hawaiian rainforests. *Remote Sens.* **2012**, *4*, 2510–2529.
33. Fyfe, S.K. Spatial and temporal variation in spectral reflectance: Are seagrass species spectrally distinct? *Limnol. Oceanogr.* **2003**, 464–479.
34. SPECCHIO. Online Spectral Database. Available online: <http://www.specchio.ch> (accessed on 11 August 2015).
35. Clark, R.N.; Roush, T.L. Reflectance spectroscopy: Quantitative analysis techniques for remote sensing applications. *J. Geophys. Res.* **1984**, *89*, 6329–6340.
36. Price, J.C. How unique are spectral signatures? *Remote Sens. Environ.* **1994**, *49*, 181–186.
37. Jacquemoud, S.; Verhoef, W.; Baret, F.; Bacour, C.; Zarco-Tejada, P.J.; Asner, G.P.; Francois, C.; Ustin S.L. PROSPECT + SAIL models: A review of use for vegetation characterization. *Remote Sens. Environ.* **2009**, *113*, S56–S66.
38. Homayouni, S.; Roux, M. Hyperspectral Image analysis for material mapping using spectral matching. In Proceedings of ISPRS Congress 2004, Istanbul, Turkey, 12–23 July 2004.
39. Kruse, F.A.; Lefkoff, A.B.; Boardman, J.B.; Heidebrecht, K.B.; Shapiro, A.T.; Barloon, P.J.; Goetz, A.F.H. The Spectral Image Processing System (SIPS)—Interactive visualization and analysis of imaging spectrometer data. *Remote Sens. Environ.* **1993**, *44*, 145–163.
40. International Organization for Standardization (ISO). *Geographic Information—Metadata*; International Organization for Standardization: Geneva, Switzerland, 2003.
41. Mac Arthur, A.; Alonso, L.; Malthus, T.; Moreno, J. Spectroscopy field strategies and their effect on measurements of heterogeneous and homogeneous earth surfaces. In Proceedings of the 2013 Living Planet Symposium, Edinburgh, UK, 9–13 September 2013.
42. Mac Arthur, A.; MacLellan, C.; Malthus, T.J. The fields of view and directional response functions of two field spectroradiometers. *IEEE Trans. Geosci. Remote Sens.* **2012**, *50*, 3892–3907.
43. Salisbury, J.W. *Spectral Measurements Field Guide*; Tech. Rep. ADA362372; Defense Technology Information Centre: Fort Belvoir, VA, USA, 1998.
44. Jonkheere, I.; Fleck, S.; Nackaerts, K.; Muys, B.; Coppin, P.; Weiss, M.; Baret, F. Review of *in-situ* methods of leaf area index determination. Part I. Theories, sensors and hemispherical photography. *Agric. For. Meteorol.* **2004**, *121*, 19–35.
45. Gitelson, A.A. Nondestructive estimation of foliar pigment (chlorophylls, carotenoids, and anthocyanins) contents. In *Hyperspectral Remote Sensing of Vegetation*; Thenkabail, A., Lyon, P.S., Huete, J.G., Eds.; CRC Press: Boca Raton, FL, USA, 2011; pp. 141–166.
46. Colombo, R.; Busetto, L.; Meroni, M.; Rossini, M.; Panigada, C. Optical remote sensing of vegetation water content. In *Hyperspectral Remote Sensing of Vegetation*; Thenkabail, A., Lyon, P.S., Huete, J.G., Eds.; CRC Press: Boca Raton, FL, USA, 2011; pp. 227–244.

47. Schmidt, K.S.; Skidmore, A.K. Smoothing vegetation spectra with wavelets. *Int. J. Remote Sens.* **2004**, *25*, 1167–1184.
48. García Novo, F.; Marín Cabrera, C. *Doñana: Agua y Biosfera*; Ministerio de Medio Ambiente: Sevilla, España, 2005.
49. Muñoz Reinoso, J.C.; García Novo, F. Multiscale control of vegetation patterns: The case of Doñana (SW Spain). *Lands. Eco.* **2005**, *20*, 51–61.
50. Zunzunegui, M.; Díaz Barradas, M.C.; Ain-Lhout, F.; Clavijo, A.; García Novo, F. To live or to survive in Doñana dunes: Adaptive responses of woody species under a Mediterranean climate. *Plant Soil* **2005**, *273*, 77–89.
51. Gratani, L.; Varone, L. Adaptive photosynthetic strategies of the Mediterranean maquis species according to their origin. *Photosynthetica* **2004**, *42*, 551–558.
52. Ain-Lhout, F. Seasonal differences in photochemical efficiency and chlorophyll and carotenoid contents in six Mediterranean shrub species under field conditions. *Photosynthetica* **2004**, *42*, 309–407.
53. Chen, J.M.; Cihlar, J. Quantifying the effect of canopy architecture on optical measurements of leaf area index using two gap size analysis methods. *IEEE Trans. Geosci. Remote Sens.* **1994**, *33*, 777–787.
54. Sweet, J.; Granahan, J.; Sharp, M. An objective standard for hyperspectral image quality. In Proceedings of AVIRIS Workshop, Jet Propulsion Laboratory, Pasadena, CA, USA, 23–25 February 2000.
55. Jimenez, M.; Pou, A.; Díaz-Delgado, R. Cartografía de especies de matorral de la Reserva Biológica de Doñana mediante el sistema hiperespectral aeroportado INTA-AHS: Implicaciones en el seguimiento y estudio del matorral de Doñana. *Revis. de Teledetec.* **2011**, *36*, 98–102.